

# Modeling of bioethanol production through glucose fermentation using *Saccharomyces cerevisiae* immobilized on sodium alginate beads

Astrilia Damayanti, Zuhriyan Ash Shiddieqy Bahlawan & Andri Cahyo Kumoro |

To cite this article: Astrilia Damayanti, Zuhriyan Ash Shiddieqy Bahlawan & Andri Cahyo Kumoro | (2022) Modeling of bioethanol production through glucose fermentation using *Saccharomyces cerevisiae* immobilized on sodium alginate beads, Cogent Engineering, 9:1, 2049438, DOI: [10.1080/23311916.2022.2049438](https://doi.org/10.1080/23311916.2022.2049438)

To link to this article: <https://doi.org/10.1080/23311916.2022.2049438>



© 2022 The Author(s). This open access article is distributed under a Creative Commons Attribution (CC-BY) 4.0 license.



Published online: 24 Mar 2022.



Submit your article to this journal [↗](#)



View related articles [↗](#)



View Crossmark data [↗](#)



Received: 22 November 2021  
Accepted: 25 February 2022

\*Corresponding author: Andri Cahyo Kumoro, Department of Chemical Engineering, Faculty of Engineering, Universitas Diponegoro, Soedarto, SH Semarang, Indonesia  
E-mail: [andri.kumoro@che.undip.ac.id](mailto:andri.kumoro@che.undip.ac.id)

Reviewing editor:  
Harvey Arellano-Garcia,  
Brandenburgische Technische  
Universität Cottbus-Senftenberg,  
Germany

Additional information is available at  
the end of the article

## CHEMICAL ENGINEERING | RESEARCH ARTICLE

# Modeling of bioethanol production through glucose fermentation using *Saccharomyces cerevisiae* immobilized on sodium alginate beads

Astrilia Damayanti<sup>1</sup>, Zuhriyan Ash Shiddieqy Bahlawan<sup>2</sup> and Andri Cahyo Kumoro<sup>2\*</sup>

**Abstract:** As a response to the increasing demand for ethanol as a renewable energy source, the design of a bioreactor to facilitate efficient glucose fermentation by *Saccharomyces cerevisiae* is very essential. Although a number of mathematical models that gave some parameters used for bioreactor design can be found in the literature, only a few models were designated for fermentation using immobilized *S. cerevisiae*. This study aimed to develop an unstructured fermentation kinetics model based on the mass transfer phenomena and the Monod equation to describe the rate of glucose consumption, glucose concentration on the bead surface, yeast cell growth, and ethanol concentration. Four ordinary differential equations obtained from the model development were solved simultaneously using fourth order Runge-Kutta with the help of MATLAB software. The accuracy of the model was verified with the experimental data collected from the relevant literature with the average error (%) of the variation of loading yeast mass, pH, and temperature were 5.12–10.08, 3.63–7.95, and 5.35–11.87, respectively. Seven adjustable kinetic parameters were also successfully obtained for a quantitative description of bioethanol production from fermentation of glucose employing *S. cerevisiae* immobilized on sodium alginate beads. The simulation results proved that the proposed model can accurately predict the concentration of glucose and ethanol in the fermentation broth, concentration of glucose on the alginate beads surface, and yeast cell concentration. Hence, the model can be potentially applied for the design of a larger



Andri Cahyo Kumoro

### ABOUT THE AUTHOR

Prof. Andri Cahyo Kumoro, PhD is an active full professor in the Department of Chemical Engineering, Faculty of Engineering, Universitas Diponegoro . Jl. Prof. H. Soedarto, SH Semarang, Indonesia 50275. His main research interest is in the bioprocessing of biomass residues into fuel, food and nutraceuticals

### PUBLIC INTEREST STATEMENT

A fermentation kinetics model based on mass transfer phenomena and Monod equations to describe glucose consumption rate, glucose concentration on sodium alginate beads surface, yeast growth, and ethanol concentration. This paper reports guess the parameters on the variation of loading yeast mass, temperature, and pH based on the smallest error function of time (hours) on the concentration of consumption of glucose, ethanol, and glucose on the surface of the sodium alginate beads. The result will be useful for developing of conception in the bioreactor with immobilized yeast *Saccharomyces cerevisiae* on sodium alginate technologies.

scale batch bioreactor for glucose fermentation using *S. cerevisiae* immobilized on sodium alginate beads for ethanol production.

**Subjects:** Adsorption Science; Biochemical Engineering; Biotechnology

**Keywords:** ethanol; thin film model; Monod; yeast; mass transfer; kinetics

## 1. Introduction

The continuous development of industrialization and transportation activities around the world has led to an incredible annual increase in fossil energy consumption by 2% to 3% per year, which triggers rapid fossil fuel resources depletion (Azhar & Abdulla, 2018). To respond to this continuous decline of fossil fuel reserves, alternatives of energy sources have to be renewable, sustainable, environmentally benign, affordable, safe, and convenient (Bušić et al., 2018; Hossain et al., 2017). As the most popular alternative to gasoline, ethanol has gained remarkable attention from researchers, which lead to the rapid development of microbial ethanol production (Rastogi & Shrivastava, 2017). Various *microorganisms*, such as *Saccharomyces cerevisiae* (Azhar et al., 2017), *Saccharomyces pastorianus* (Harcum & Caldwell, 2020), *Saccharomyces bayanus* (Gil & Maupoey, 2018), *Kluyveromyces marxianus* (Murari et al., 2019), *Clostridium sp.* and *Zymomonas mobilis* (Beltran et al., 2020) have been proven to be the appropriate candidates to produce ethanol in commercial-scale. Naturally, both *S. cerevisiae* as the mesophilic and *K. marxianus* as the thermotolerant yeasts are acidophilic *microorganisms*. Therefore, they can grow well if the conditions are under an acidic environment with a pH range of 4.0 to 6.0, high and low temperatures, the presence of oxygen, and the type of yeast strain (Tkavc et al., 2018).

The simplicity of batch fermentation provides easy operation and control, low investment costs, and high yield for ethanol production from glucose (S. Y. Lee et al., 2011). This process is reported to be influenced by fermentation time (Chen et al., 2014), temperature (Hossain et al., 2017; Alberti et al., 2017), pH (Azhar et al., 2017; Silva-Illanes et al., 2017) and inoculum loading (Azhar et al., 2017; Alberti et al., 2017). The optimum conditions for glucose fermentation using *S. cerevisiae* to obtain maximum ethanol production were at 25°C to 40°C (Tofighi et al., 2014; Ünal et al., 2020), pH 5 (Mishra et al., 2016), and inoculum loading of  $1 \times 10^8$  cells/mL for 48 hours (Nuanpeng et al., 2018). Fermentation employing immobilized yeast cells is more advantageous than conventional fermentation using free yeast cells, which includes a larger biomass concentration in the reactor and higher cell's activity (Chacón-Navarrete et al., 2021; Todhanakasem et al., 2020), higher ethanol productivity, and yield, lower operating cost due to cell reuse for subsequent fermentation cycles, and low tendency to be contaminated (Duarte et al., 2013). Ethanol production using *Z. mobilis* in an immobilized cell reactor (ICR) was nearly two times that carried out in a free cell bioreactor (Nordmeier & Chidambaram, 2018).

The application of biofilm reactor has been studied to enhance the economics and performance of the fermentation process for ethanol production (Karagoz et al., 2019). Fermentation using immobilized cells has been investigated to eliminate substrate and product inhibitions caused by their high concentrations, which subsequently enhance yield and productivity. However, cells entrapped in the porous matrices are exposed to a condition, which is largely different from the bulk solution, since immobilized cell systems are composed of the cells, the support material, and the void spaces in a fluid-filled support structure. Generally, the limited supply of nutrients to cells in immobilized cells occurs due to the absence of convective flow inside the beads so that nutrients are received by cells only by diffusion (Riley et al., 1996). Several researchers investigated the immobilized cell system on

mass transfer on the cell growth rate, inhibitory effects of substrates and/or products, and product formation (Žur et al., 2016).

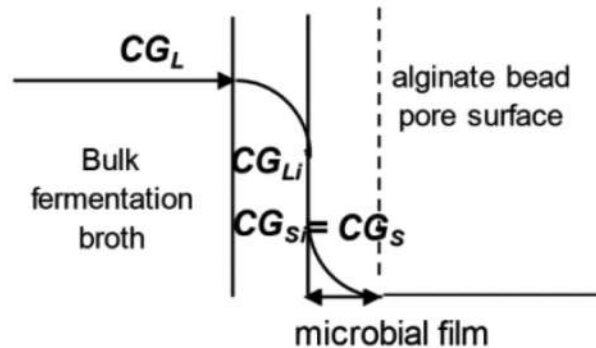
Mathematical simulations are proven to be dynamic tools for evaluating the fermentation processes that significantly reduce the cost for carrying out experiments, especially for the design, control, and scale-up (Mears et al., 2017). The accuracy of the simulation itself is strongly dependent on the appropriateness of the underlying mathematical model applied for the estimation of the responses of a given system to environmental changes and operating conditions. Therefore, the mathematical models should correctly describe the mechanisms of the processes under consideration. For the aims of fermentation simulation, kinetic models based on the mass balance of the substrate and targeted product in the bioreactor are generally applied. As a response to the rising interest in an alcoholic fermentation for commercial application, numerous kinetic models of freely suspended cells for both batch and continuous operation have been proposed (Kyriakou et al., 2019). However, no kinetic models can be expected to be directly suitable to a real process condition. Hence, mathematical modeling should be initiated from the simplest type, but it must be then improved and extended until it satisfactorily describes the real process mechanisms. The most fundamental aspect of unstructured models of microbiological processes is the approximation of time-varying cell concentrations or high substrate concentrations rather than the saturation constant (Manheim et al., 2019). In fact, the control models for the common commercial applications are usually derived from the simple—unstructured models because the computation process will help to look for the appropriate value of the adjustable parameters based on the response of the system to any given disturbances. The mathematical model proposed in this paper is thus developed based on the fundamental mass transfer and microbiological processes by immobilized *S. cerevisiae*. Glucose consumption, ethanol production, and growth pattern of immobilized yeast cells in sodium alginate beads were evaluated from a study of the influential fermentation conditions in a stirred batch fermentation (Kumoro et al., 2021).

### **1.1. Mathematical model development**

In order to gain a better understanding of the phenomena and to generalize the results obtained, it is necessary to conduct a kinetic study supported by mathematical modeling. A simplified mass-balance mathematical model can be developed by considering only the kinetic rates of the controlling reaction processes, which involve the substrate consumption for biomass and product formation, ethanol production, and yeast growth. In the fermentation process, the biofilm is attached to the Na-alginate beads as the immobilizing media, and the glucose is fed to the reaction flask following a batch system. The glucose in the fermentation broth is converted to ethanol by the yeast in the biofilm and continuously released from the yeast cells. Kinetics models to quantitatively describe the process are proposed. Theoretically, for the case of fermentation involving immobilized cells, there is the additional influence of the mass transfer resistances on the process dynamics. Hence, the model can be well represented by the inclusion of both internal diffusion and convective mass transfer at the surface of the solid matrix containing immobilized yeasts to the model mass balance equations. However, it is also important to consider that the structure of 2% (w/v) Na-alginate beads was strong enough and no observable leakage of cells from the beads into the bulk of fluid was found in the immobilized cell reactor (ICR) column (Najafpour et al., 2004). They also reported that yeast cells grew on the surface of the outer beads at which apparent active sites were still observed upon 72 hours of fermentation in the ICR suggesting the sufficient availability of the yeast for ethanol production without diffusion problems.

Metabolic flux analysis (MFA) is a powerful analytical method employing a rigorous optimization procedure to measure the quantity of the intracellular metabolic fluxes resulted from all recognized catalytic and transcriptional interactions. Although the MFA is basically

**Figure 1.** The mass transfer mechanism of glucose from the fermentation broth to the biofilm.



performed based on the stoichiometry of the metabolic reactions and the mass balances of the intracellular metabolites, which are assumed to occur under pseudo-steady state conditions, two methods are generally used to study the metabolic flux presents in a biological system, namely the C-based flux analysis and constraint-based flux analysis (S. Y. Lee et al., 2011). In this work, the MFA was used to determine the main metabolic pathway based on an optimal criterion (maximum growth) using the stoichiometric constraint and the following general assumptions:

1. The concentration and movement of the substrate in the reaction flask are uniform.
2. The fermentation system is pseudo-isothermal.
3. The biofilm thickness increases as time progresses.

The mechanism of the combined mass transfer and biochemical reaction process is then proposed as follows (Figure 1).

The values of glucose concentration at the yeast cells biofilm surface grown on the alginate bead particles pore surface can be predicted by means of its mass balance similar to the case of a single biocatalyst particle. For this objective, the following assumptions were taken into account:

- (1) the yeast cells are uniformly distributed inside the alginate bead particles pores with low concentration and they are involved in the biochemical reactions to convert glucose into ethanol without any kind of physical limitation (Azhar et al., 2017)
- (2) the effective diffusion coefficient for ethanol is far higher than that of glucose (Landaeta et al., 2019), and that there were no substrate and product diffusion limitations in the alginate bead pores suggesting that their concentration within the bead pores is uniform (Mishra et al., 2016; Saha et al., 2019).
- (3) there are no physical or chemical interactions between the substrate or products and the alginate bead particles.
- (4) Ethanol remains in the fermentation broth during the fermentation process because it is highly soluble in water and does not accumulate in the immobilized yeast cells (Zentou et al., 2019).

Based on the previous observation that internal diffusion of glucose within the alginate beads pores is very rapid (Lee & Mooney, 2012), the pores should always be filled with

glucose solution. Therefore, glucose from the bulk of the fermentation broth is transferred to the surface of the biofilm through a liquid film via a diffusion mechanism across the liquid-biofilm interface.

The rate of glucose mass transfer from the bulk of fermentation broth through the liquid film can be approximated by equation (1; Bird et al., 2015):

$$r_{Gm} = -\frac{dC_{G_L}}{dt} = k_L \cdot a_m (C_{G_L} - C_{G_{Li}}) \quad (1)$$

The glucose molecules then diffuse into the inner part of the biofilm. Since the rate of biofilm thickness increase is much slower than the rate of substrate consumption, the system conditions can be assumed to be at a quasi-steady state for short periods of time. Therefore, it is plausible to assume that the immobilized cell aggregation is at a quasi-steady state and all the cells inside the biofilm are in the same physiological phase by which an average kinetic constant can be applied for the microbial phase (yeast cells). While diffusing through the biofilm, some glucose is converted into ethanol by the yeast cells residing in the biofilm. The rate of the glucose consumption by yeast cells can be approximated by Monod's equation (Sivarathnakumar et al., 2019):

$$r_G = \mu = \mu_{max} \cdot \frac{C_{G_S}}{C_{G_S} + K_S} \quad (2)$$

The  $K_S$  and  $\mu_{max}$  terms denote the Monod constant or half-saturation constant of growth kinetics and maximum-specific growth rate, respectively. Najafpour et al. (2004) found that the values of the Monod's constant and maximum specific growth rate were 2.23 g/L and 0.35 g/(L.h), respectively. In the existence of alginate beads, yeast cells biofilm, and counter-diffusion, the effective diffusion coefficient for ethanol is far higher than that of glucose (Estape et al., 1992). Therefore, ethanol as the product of glucose conversion can be immediately released from the yeast cells resulting in negligible ethanol inhibition. In addition, when ethanol tolerant yeast is employed for the fermentation, the effect of product inhibition will also be insignificant Kostov et al., 2012).

Because glucose diffusion through the alginate beads pores is relatively fast (A. Damayanti et al., 2021), its concentration in the bulk liquid of Na-alginate bead pores value is considered to be uniform ( $C_{G_L}$ ), while glucose concentration at the biofilm surface  $C_{G_S}$  varies with fermentation time. The yeast cells can be assumed to grow proportional to the amount of glucose consumed as substrate. As a result, the thickness of the biofilm increases. However, because biofilm thickness ( $\delta$ ) is relatively thin (Zakhartsev & Reuss, 2018), so its geometry still can be assumed as a slab.

### 1.2. The mass balance of glucose on the biofilm on Na-alginate beads surface

Glucose mass balance can be performed by involving ethanol inhibition of the Hinshelwood model.

Rate of mass input—Rate of mass output—Rate of mass reaction = Rate of mass accumulation

$$k_{La}(C_{G_L} - C_{G_{Li}}) - 0 - a \cdot \delta \cdot r_G = \frac{dC_{G_S}}{dt} \quad (3)$$

$$\frac{dCG_S}{dt} = k_L \cdot a_m \cdot (CG_L - CG_{Li}) - \frac{1}{Y_x} \cdot \frac{dX}{dt} - \frac{1}{Y_E} \cdot \frac{dCE_L}{dt} \quad (4)$$

In equation (1) and equation (4),  $CG_{Li}$  is the concentration of glucose in the liquid phase that is in equilibrium with glucose concentration in the surface of biofilm ( $CG_{Si}$ ). According to the substance partition concept, which is the Henry's type equation (Bird et al., 2015):

$$CG_{Li} = H_s \cdot CG_{Si} \quad (5.a)$$

Based on the assumption that the yeast cells biofilm is very thin (Zakharov & Reuss, 2018), the value of  $CG_{Si}$  is approximately equal to  $CG_S$ , so equation (5.a) becomes:

$$CG_{Li} = H_s \cdot CG_S \quad (5.b)$$

Hence, equation 5(b) is substituted to equation (1) and (4) becomes:

$$\frac{dCG_L}{dt} = -k_L \cdot a_m \cdot (CG_L - H_s \cdot CG_S) \quad (6)$$

$$\frac{dCG_S}{dt} = k_L \cdot a_m \cdot (CG_L - H_s \cdot CG_S) - \frac{1}{Y_x} \cdot \frac{dX}{dt} - \frac{1}{Y_E} \cdot \frac{dCE_L}{dt} \quad (7)$$

Since the rate of yeast cell growth ( $r_X$ ) is proportional to the rate of glucose consumption ( $r_G$ ), the rate of yeast growth can be estimated by:

$$r_X = \frac{dX}{dt} = \mu \cdot X = \mu_{max} \cdot \left( \frac{CG_S}{CG_S + K_S} \right) \cdot (1 - K_{EX} \cdot CE_{SL}) \cdot X \quad (8.a)$$

However, if no product (ethanol) inhibition to the yeast cell growth, equation (8.a) can be simplified to:

$$r_X = \frac{dX}{dt} = \mu \cdot X = \mu_{max} \cdot \left( \frac{CG_S}{CG_S + K_S} \right) \cdot X \quad (8.b)$$

However,  $CG_S$  cannot be directly measured from experiments. So, their values should be calculated from the  $CG_L$  value as the measurable quantity in the fermentation process.

In a closed fermentation system where cell growth is the sole process that influences the microbial cell concentration, the cell growth rate ( $r_X$ ) is equivalent to the rate of change of cell concentration. By establishing the microbial film thickness at a specified time is  $\delta$ , the rate of the yeast cells mass (X) change is:

$$\frac{dX}{dt} = r_X \cdot a \cdot \delta \quad (9.a)$$

The mass of the microorganisms  $X = \rho \cdot V$ , where  $\rho$  is mass of yeast cells per volume of microbial film (or density) and  $V$  is the volume of the microbial film, equation (9.a) becomes:

$$\frac{d(\rho \cdot a_m \cdot \delta)}{dt} = Y_x \cdot r_G \cdot a_m \cdot \delta \quad (9.b)$$

where  $Y_{X/S}$  is the yield coefficient that defines the ratio of the yeast cell's mass growth to the mass of glucose consumed. Since the surface area of the microbial film ( $a_m$ ) and density of yeast cells are relatively constant, equation (9.b) can be simplified into the equation (9.c):

$$\frac{d\delta}{dt} = Y_{X/S} \cdot \frac{\delta}{\rho} \cdot \mu_{max} \cdot \frac{CG_S}{CG_S + K_S} \tag{9.c}$$

### 1.3. Mass balance of ethanol in the bulk fermentation broth

The specific growth kinetics, incorporating the Monod dependence on the substrate and the growth inhibition by the ethanol as a product can be written using the Hinshelwood model:

Rate of mass input—Rate of mass output—Rate of mass reaction = Rate of mass accumulation

$$0 - 0 + a \cdot \delta \cdot r_E = \frac{dCE_L}{dt} \tag{10}$$

$$\frac{dCE_L}{dt} = Y_{E/S} \cdot a_m \cdot \delta \cdot \mu_{max} \cdot \frac{CG_S}{CG_S + K_{SE}} \cdot (1 - K_{EE} \cdot CE_L) \cdot X \tag{10.a}$$

$$\frac{dCE_L}{dt} = q_{max} \cdot \left( \frac{CG_S}{CG_S + K_{SE}} \right) \cdot (1 - K_{EE} \cdot CE_L) \cdot X \tag{10.b}$$

where  $K_{EE}$  and  $CE_L$  are respectively the inhibition constants for the ethanol and the concentration for the ethanol in the bulk fermentation broth. Hence, if ethanol production is not inhibited by ethanol concentration (Vives et al., 1993), Equation (10.b) can be simplified into:

$$\frac{dCE_L}{dt} = q_{max} \cdot \left( \frac{CG_S}{CG_S + K_{SE}} \right) \cdot X \tag{10.c}$$

The ethanol inhibition during fermentation for immobilized yeast cells can be represented by Luong's model (Zentou et al., 2021):

$$\mu = \mu_{max} \cdot \left( 1 - \frac{CE}{CE_c} \right)^n \tag{11}$$

where  $\mu$  is the specific fermentation rate ( $h^{-1}$ ),  $\mu_{max}$  is the maximum specific fermentation rate ( $h^{-1}$ ),  $CE$  is the ethanol concentration ( $g \cdot dm^{-3}$ ),  $CE_c$  is the critical ethanol concentration at which fermentation is stop ( $g \cdot dm^{-3}$ ) and  $n$  is the so-called toxic power of ethanol (dimensionless). Vives et al. (1993) observed that the value of  $\mu_{max} \cdot CE_c$ , and  $n$  for *S. cerevisiae* cells immobilized on Ca-alginate beads are 1.02 ( $h^{-1}$ ), 98.5 (g/L) and 0.59, respectively.

Thus, the mathematical models representing the conversion of glucose using yeast cells immobilized on Na-alginate beads are the set of equations (6), (7), (8.b), and (10.c) can be solved simultaneously using the initial conditions:  $CG_L(0) = CG_{L0}$ ,  $CG_S(0) = 0$ ,  $CE_L(0) = 0$ , and  $\delta(0) = 0$ . The accuracy of the proposed model can further be verified with the data obtained from the experiment.



## 2. Materials and methods

### 2.1. Chemicals and microorganisms

The chemicals used in this study were the same as those previously used by Kumoro et al. (2021). Glucose solution at a concentration of 172 g/L was carefully prepared from glucose powder (Sigma-Aldrich). Instant Dry Yeast ("Fermipan", Indonesia), which was sold as 0.5183 g per tablet containing  $1 \times 10^8$  cells/mL was used as the original source of *S. cerevisiae*.

### 2.2. Preparation of yeast cell suspension

The cells suspension employed in this study was prepared according to the protocol described by Kumoro et al. (2021). A carefully prepared (50 mL) growing media (a mixture of 5 g/L peptone and 10 g/L glucose) was introduced in a 250 mL Erlenmeyer flask. Upon autoclaving of the growing media at 121°C for 15 minutes for sterilization, the dry yeast (0.25, 0.5, 0.75, and 1 g) was added to the sterile solution and followed by aseptic mixing in an orbital shaker operated at 150 rpm and ambient temperature for 24 hours. Then, 50 mL sterile water was added to the resulting cell suspension to obtain 100 mL dilute suspension and were ready for further use.

### 2.3. Preparation of immobilized yeast cells

The immobilized yeast cells employed in this study were prepared according to the protocol described by Kumoro et al. (2021). The cell suspension obtained from centrifugation was added to a 2% (w/v) alginate solution in a ratio (w/v) of 1:1 (A., Sarto Damayanti et al., 2020). Then the mixture was introduced dropwise into 0.1 M  $\text{CaCl}_2$  solution at 30°C with an inflated syringe. The beads formed in the  $\text{CaCl}_2$  solution were stored for 20 hours at 4°C before use.

### 2.4. Preparation of ethanol production using glucose with immobilized yeast cells

Nutrients as the fermentation medium used in this study were the same as those previously used by Kumoro et al. (2021). The nutrients consist of 5 g/L ammonium sulfate, 2.5 g/L yeast extract, 6 g/L magnesium sulfate, and 1.7 g/L yeast nitrogen base.

### 2.5. Analysis Model

The data measured during the FERMENTATION process was the concentration of glucose and ethanol dissolved in the solution at various times. Parameters that can be set in the mathematical model are  $K_{La}$ ,  $H_S$ ,  $\mu_{max}$ ,  $K_{SX}$ ,  $q_m$ ,  $K_{SE}$ ,  $Y_{X/S}$ , and  $Y_{E/S}$ . To obtain the values of these parameters were solved with the help of the MATLAB software. The parameter value is obtained through the calculation of % error (equation 12-14). Furthermore, curve fitting between the observed data and calculated results was also conducted.

$$\% \text{Ethanol Conc. Error} = \sum_{i=1}^n \text{Abs} \left( \frac{\text{measured data}_i - \text{measured calculation}_i}{\text{measured data}_i} \right) \times 100\% \quad (12)$$

$$\% \text{Glucose Conc. Error} = \sum_{i=1}^n \text{Abs} \left( \frac{\text{measured data}_i - \text{measured calculation}_i}{\text{measured data}_i} \right) \times 100\% \quad (13)$$

$$\% \text{ average error} = \left( \frac{\text{Ethanol Conc. error} + \text{Glucose Conc. error}}{2} \right) \quad (14)$$

Figure 2. Comparison of calculated glucose, glucose bead interface, and ethanol concentrations as a function of time and yeast mass loading (g dry) (a) 0.25, (b) 0.5, (c) 0.75, and (d) 1.0 during glucose fermentation using *S. cerevisiae* immobilized on sodium alginate beads.

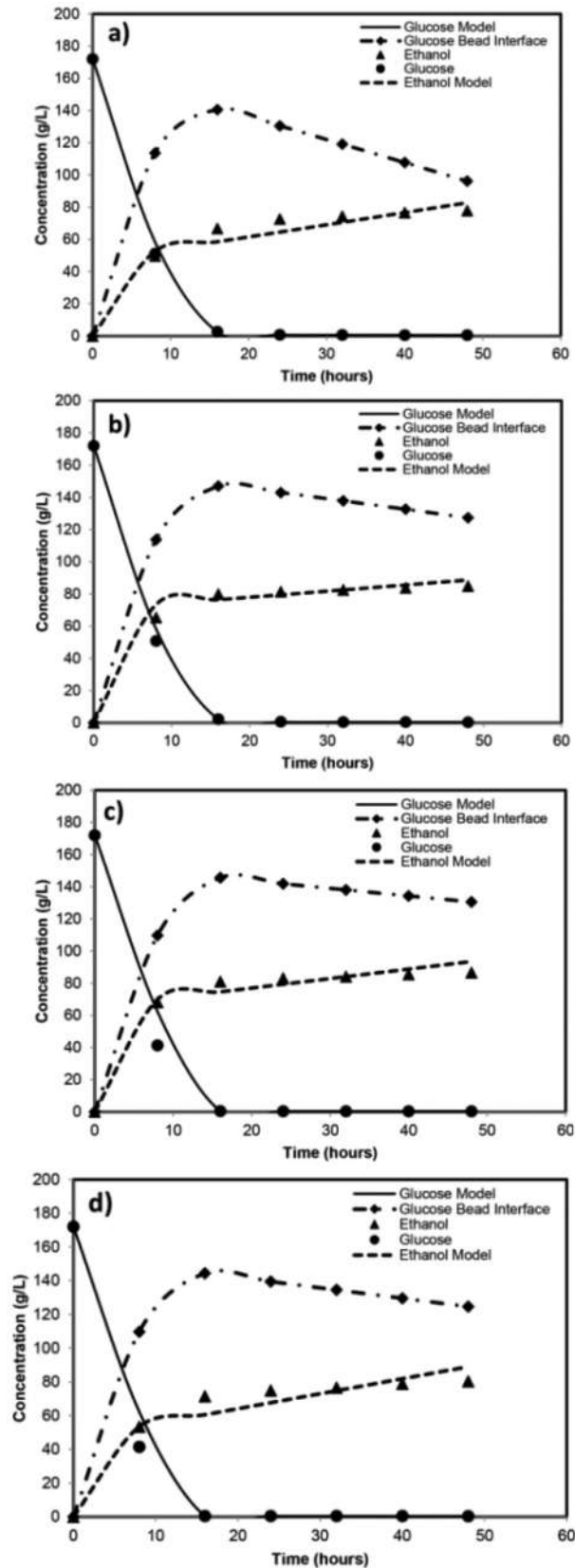


Figure 3. Comparison of calculated glucose, glucose bead interface, and ethanol concentrations as a function of time and temperature (oC) (a) 25, (b) 30, (c) 35, and (d) 40 during glucose fermentation using *S. cerevisiae* immobilized on sodium alginate beads.

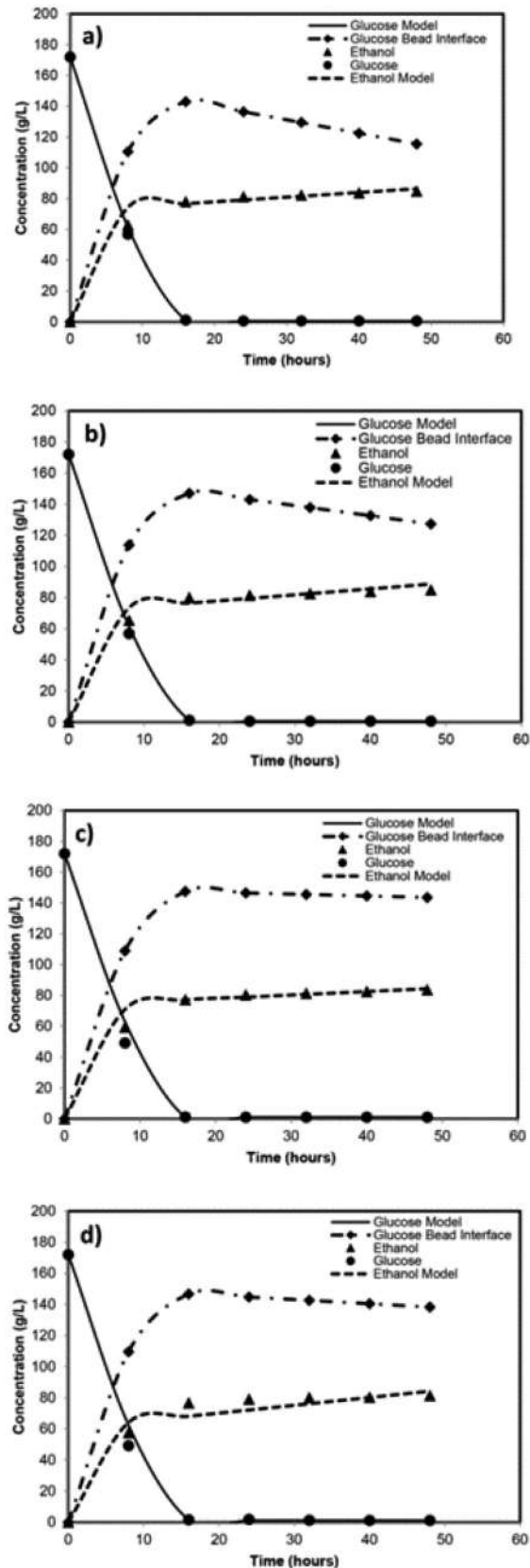
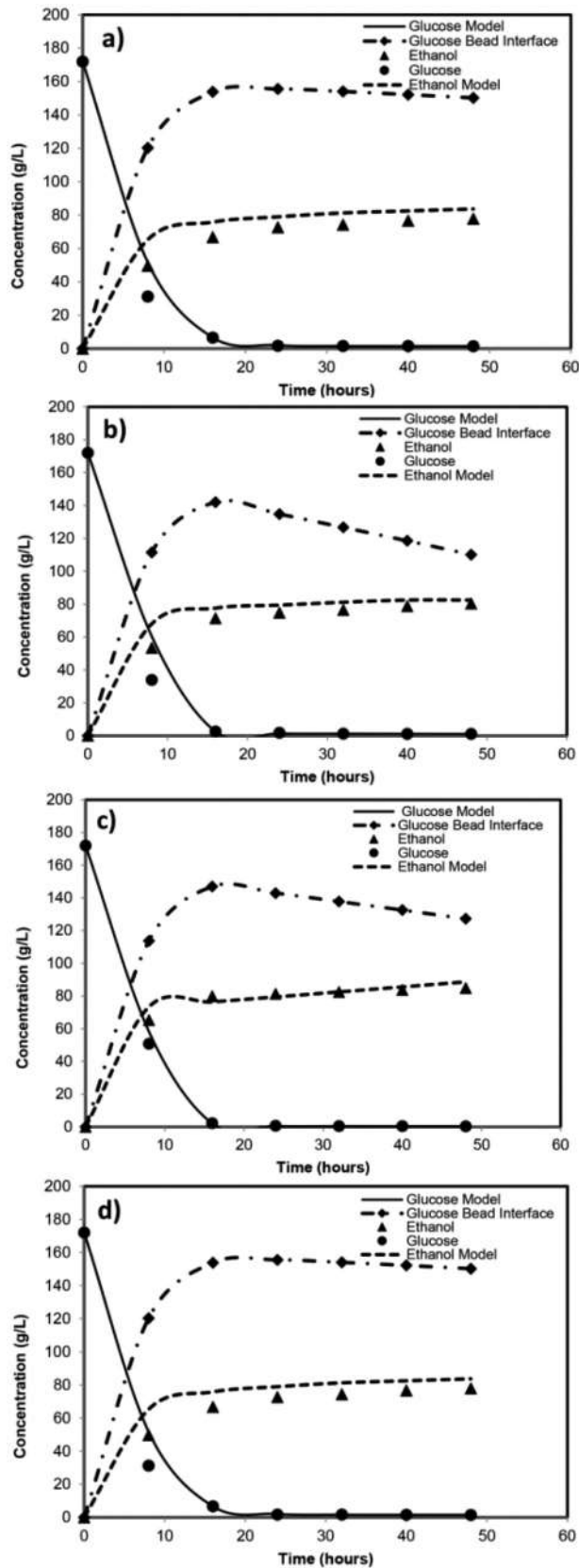


Figure 4. Comparison of calculated glucose, glucose bead interface, and ethanol concentrations as a function of time and pH (a) 3.0, (b) 4.0, (c) 5.0, and (d) 6.0 during glucose fermentation using *S. cerevisiae* immobilized on sodium alginate beads.



### 3. Results and discussion

#### 3.1. Effect of mass yeast load

The optimized adjustable parameters obtained from the mathematical modeling along with the average absolute errors for both glucose and ethanol concentrations, and their mean values at various yeast mass loading, temperature, and pH for glucose fermentation using immobilized *S. cerevisiae* on sodium alginate beads are presented in Table 1, 2, and 3, respectively. Accordingly, the corresponding calculated and experimental data (glucose and ethanol concentrations in the bulk fermentation broth and glucose concentration at the sodium alginate beads surface) are depicted in Fig. 2, 3, and 4.

Table 1 shows that a higher yeast mass loading (g) resulted in a higher ethanol yield ( $Y_{E/S}$ ) value although no significant difference of yeast mass on glucose yield ( $Y_{X/S}$ ) was observed. The close values of  $Y_{X/S}$  indicate that the *S. cerevisiae* strain used in the fermentation effectively used the glucose as the substrate to grow and multiply their cell number. From their modeling, Aguilar-Uscanga et al. (2011) also revealed that yeast mass on glucose yield coefficient ( $Y_{X/S}$ ) decreased when fermentation was performed using a higher yeast mass loading. In addition, the close values of mass transfer coefficient ( $k_{La}$ ) and equilibrium constant ( $H_S$ ) across the microbial film confirmed the assumption that the microbial films were extremely thin. However, an excessive yeast mass loading (beyond 0.5) led to a drastic reduction of the maximum yeast growth rate ( $\mu_{max}$ ) and maximum-specific ethanol production rate ( $q_{max}$ ), which can be due to the extremely tough competition between the yeast cells. The results are in accordance with  $\mu_{max}$  values reported by Woo et al. (2014) and J. S. Lee et al. (2013) where a lower initial glucose concentration for a given *S. cerevisiae* BY4741 and *S. cerevisiae* NK28 mass loading caused higher  $\mu_{max}$  values. The higher average error values between the calculated glucose and ethanol concentrations and those obtained from experiments were obvious to fermentation using a higher yeast mass loading. This increase can be clearly seen in Figure 2.

As presented in Figure 2, all the corresponding experimental data and calculation results exhibit the same trend. Glucose concentrations in the fermentation and became close to zero at 16 hours because glucose rapidly entered the Na-alginate bead pores and was followed by a quick diffusion to the microbial film. Thiele modulus ( $\phi$ ) can be used to identify the effect of internal diffusion on the biochemical reaction rate (Galaction et al., 2010). Vives et al. (1993) also reported that the observable Thiele modulus ( $\phi$ ) values for both glucose and ethanol were always in the range between  $1 \times 10^{-3}$  to  $6 \times 10^{-2}$ , which confirm that there were no internal and external diffusion limitations in the alginate beads. Scott et al. (1989) also found that the diffusivity coefficient of glucose solution with 10–200 g/L concentration to 2 mm alginate beads at 30°C ranged between  $6.0 \times 10^{-6}$  to  $6.8 \times 10^{-6}$   $\text{cm}^2 \cdot \text{s}^{-1}$ . The diffusivity coefficient of ethanol in water was  $1.98 \times 10^{-5}$   $\text{cm}^2 \cdot \text{s}^{-1}$ . This condition denotes that the mass transfer rate in the alginate beads with entrapped cells is very fast relative to the fermentation rate. However, this glucose is also simultaneously consumed by *S. cerevisiae* cells in the microbial film to support their growth and production of ethanol. As a result, ethanol concentration increased significantly within the same period due to the conversion of glucose. Ethanol concentration continued to increase gradually until 32 hours of fermentation. Unfortunately, beyond 32 hours, ethanol concentrations became almost constant for fermentation using 0.5, 0.75, and 1.0 g dry yeast, which indicate exceptionally low ethanol production rates caused by the attenuation of glucose as substrate. The slowest glucose consumption and ethanol production rates can be observed for fermentation using 0.25 g dry yeast. Meanwhile, glucose concentration on the surface of the Na-alginate beads was almost linear in the first 8 hours of fermentation and was followed by a gradual increase to reach the maximum value at about 16 hours of fermentation. This phenomenon proved the existence of mass transfer resistance of glucose from the bulk fermentation broth to the

**Table 1. Kinetic data parameters for bioethanol production through glucose fermentation using *S. cerevisiae* immobilized on sodium alginate beads with variation loading yeast**

Loading mass yeast (g dry)	Adjustable parameters								Error (%)		Average error (%)
	$k_{La}$	$Hs$	$\mu_{max}$	$K_{SX}$	$q_{max}$	$K_{SE}$	$Y_{X/S}$	$Y_{E/S}$	Glucose conc.	Ethanol conc.	
0.25	0.250	0.0048	0.0013	67.075	0.918	0.756	0.645	0.620	4.42	5.82	5.12
0.50	0.250	0.0026	0.0011	70.502	0.233	0.909	0.632	0.717	7.02	3.69	7.02
0.75	0.259	0.0025	0.0001	80.638	0.254	6.415	0.616	1.469	9.43	3.82	6.63
1.00	0.259	0.0027	0.0001	81.548	0.286	6.189	0.614	1.686	10.08	5.97	10.08

surface of the Na-alginate beads and followed by fermentation by *S. cerevisiae* cells entrapped the pores of the Na-alginate beads. Prolong fermentation time caused a gradual reduction of glucose concentration on the surface of the Na-alginate beads because glucose is consumed by *S. cerevisiae* cells as a substrate for their growth and is converted to ethanol.

A comprehensive mathematical model of the fermentation process for ethanol production should be capable of accurately describing the phase transitions of yeast *S. cerevisiae* along the fermentation course which consists of the lag phase, exponential phase, the stationary phase, and the death phase. Figure 2 also presents good agreement between the modeling results with the experimental data that suggests the proposed model is good enough in describing the whole phenomena involved in the fermentation process using immobilized yeast cells.

As seen in Figure 2 (a), the exponential phase of ethanol concentration obtained from fermentation using the lowest yeast mass loading is the most sloping and no obvious stationary phase can be observed due to its extremely slow increase. This phenomenon can also be confirmed by the smaller value of cell growth ( $K_{SX}$ ) and ethanol production rate ( $K_{SE}$ ; Table 1). At a lower yeast mass loading, there will also be a smaller number of available yeast cells in the fermentation media, which are responsible for the slower glucose conversion to ethanol although the available glucose in the Na-alginate pores was sufficiently high.

The modeling calculation estimated that the highest ethanol concentration (93.50 g/L) was achieved when fermentation was carried out using 0.75 g yeast mass loading and an initial glucose concentration of 172 g/L for 48 hours. This value is still below the critical ethanol concentration (98.5 g/L) reported by Vives et al. (1993), where the ethanol becomes toxic to the yeast cells, potentially inhibits yeast cell growth, viability, and vitality, increase cell death, and leads to reduce fermentation productivity and ethanol yield (Stanley et al., 2010). Ethanol also affects yeast cells metabolism and their macromolecular biosynthesis by triggering the formation of heat shock-like proteins, declining of ribonucleic acid (RNA) and protein accumulation rates, improving petite mutation's frequency, changing the metabolism, causing intracellular proteins and glycolytic enzymes denaturation, and lowering their activity (Hu et al., 2007). Therefore, under that fermentation condition, ethanol production is still not inhibited by ethanol concentration (Vives et al., 1993; Zentou et al., 2021). This modelling results also allow the extension of the fermentation period to a longer time until the ethanol concentration is close to the critical ethanol concentration.

**Table 2. Kinetic data parameters for bioethanol production through glucose fermentation using *S. cerevisiae* immobilized on sodium alginate beads with variation temperature**

Temp (°C)	Adjustable parameters								Error (%)		Average error (%)
	$k_{La}$	$H_s$	$\mu_{max}$	$K_{SX}$	$q_{max}$	$K_{SE}$	$Y_{X/S}$	$Y_{E/S}$	Glucose conc.	Ethanol conc.	
25	0.256	0.0040	0.0008	86.670	0.192	5.15	0.544	0.413	3.68	3.59	3.63
30	0.251	0.0026	0.0011	70.502	0.233	7.50	0.382	0.717	7.02	3.69	5.35
35	0.258	0.0067	0.0000	80.679	0.147	6.85	0.706	2.186	4.46	4.29	4.38
40	0.257	0.0077	0.0000	86.681	0.322	5.84	0.694	2.160	10.21	5.68	7.95

**Table 3. Kinetic data parameters for bioethanol production through glucose fermentation using *S. cerevisiae* immobilized on sodium alginate beads with variation pH**

pH	Adjustable parameters								Error (%)		Average error (%)
	$k_{La}$	$H_s$	$\mu_{max}$	$K_{SX}$	$q_{max}$	$K_{SE}$	$Y_{X/S}$	$Y_{E/S}$	Glucose conc.	Ethanol conc.	
3.0	0.251	0.0116	0.0001	71.992	0.134	2.306	0.396	1.183	18.15	1.69	9.92
4.0	0.252	0.0088	0.0011	70.154	0.226	0.911	0.374	0.894	15.02	7.99	11.51
5.0	0.251	0.0026	0.0010	70.502	0.233	0.909	0.382	0.720	7.02	3.69	5.35
6.0	0.229	0.0090	0.0010	70.159	0.225	0.911	0.374	0.896	12.55	11.19	11.87

### 3.2. Effect of temperature

If a higher initial glucose concentration is used, then a higher ethanol concentration can be expected. The relatively close values of the mass transfer coefficient ( $k_{La}$ ) and the equilibrium constant ( $H_s$ ) in the system presented in Table 2 agree with the assumption that the microbial films were very thin. Under this circumstance, the increase in temperature should not significantly affect the values of the glucose mass transfer coefficient ( $k_{La}$ ) from the fermentation broth to the pores of Na-alginate beads. In addition, the increase in temperature only slightly increased the values of the equilibrium constant. As expected, the increase in temperature significantly promoted the increase of both cell yield ( $Y_{X/S}$ ) and ethanol yield ( $Y_{E/S}$ ). Unfortunately, after the ethanol yield achieved its highest value at 35°C, a slight ethanol yield reduction was observed at 40°C. This finding is in accordance with the results reported by J. S. Lee et al. (2013) and Kuloyo et al. (2014) that the highest ethanol yield took place at a temperature of 35°C. This phenomenon was probably due to considerable yeast cell death or/and denaturation of enzymes in the yeast cells at a 40–42°C (Huang et al., 2018; Woo et al., 2014). It is also an indication that the *S. cerevisiae* strain used in the experiment was sensitive to exposure to high temperatures or less tolerant to thermal stress (Lin et al., 2021; Tofighi et al., 2014; Woo et al., 2014). The value  $\mu_{max}$  decreases because the cell begins to defend itself in order to stay alive, as a result of the depletion of the available substrate. The model also confirmed that as the fermentation temperature rose to beyond 30°C, the yeast cells were not able to multiply themselves ( $\mu_{max} = 0$ ) and substantially caused a significant reduction of the maximum ethanol production rate ( $q_{max}$ ).

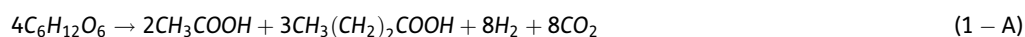
Such yeast cell death may also be the result of an increase in the accumulated poisonous substances derived from metabolic changes in the cells (Eisenberg & Büttner, 2014; Kwolek-Mirek & Zadrag-Tecza, 2014). Table 2 further describes the higher average errors between the calculated glucose and ethanol concentrations and those obtained from experiments when the fermentations were performed at higher temperatures. This increase can be clearly observed in Figure 3 where the trend of the experimental data and the simulation results are the same as that presented in Figure 2. The error of glucose concentration in both Table 2 and Figure 3 are clearly the same, where the higher the temperature, the greater the error even though the increase in error in Figure 3 only occurs at the eighth hour. The physical phenomena that can be drawn from Figure 3 are that the decrease in the glucose concentration in the fermented broth and that it becomes close to zero at the first 16 hours due to rapid glucose diffusion entering the pores of the Na-alginate beads and its further diffusion into the microbial layer. Theoretically, glucose should diffuse more rapidly at higher fermentation temperatures than at 30°C (Nikolić et al., 2012).

Although this mechanism can be harmful to the free yeast cells, the immobilization of yeast cells on Na-alginate beads has been reported to be useful in protecting the cells from the undesirable impact of high glucose concentration (Bangrak et al., 2011; Rattanapan et al., 2011). As seen in Figure 3, the glucose concentrations at the Na-alginate bead interface (g/L) at the studied temperatures were not significantly different. Figure 3 also exhibits the good agreement between the calculation results of the proposed model and the experimental data in describing the involving phenomena of the fermentation process.

As seen in Figure 3(b), the phase of the exponential concentration of ethanol obtained from the fermentation at 30°C is the most declivous and no stationary phase can be observed due to its extremely slow increase. This phenomenon can also be confirmed with the lower values of half-saturation constant of cell growth ( $K_{SX}$ ), and also both cell yield ( $Y_{X/S}$ ) and ethanol yield ( $Y_{E/S}$ ; Table 2). At this temperature, the surface of the alginate beads is still able to transfer heat into the yeast cells (Liu & Shen, 2008) that facilitating the enzymes to regulate the microbial activity to function normally. The condition became different at the higher temperatures where the  $K_{SE}$  value decreased because the regulating enzymes were no longer active due to the alteration of the tertiary structure of the cells (Phisalaphong et al., 2006). Table 3 shows the comparable values of the mass transfer coefficient ( $k_{La}$ ) and the constant equilibrium ( $H_S$ ) in the entire movie microbial at all the pH studied that confirm the assumption that the film of microbes is very thin. Although the mass transfer coefficient ( $k_{La}$ ) of glucose from the fermentation broth to the surface of the Na-Alginate beads at pH 3.0 was comparable with the fermentations at other pH values, the Henry-like equilibrium constant ( $H_S$ ) at pH 3.0 was the highest (Table 3). Hence, the consumption of glucose available in the Na-Alginate beads surface at pH 3.0 was slower than at other fermentation conditions (Figure 4 (a)).

### 3.3. Effect of pH fermentation

The increase in pH of the fermentation broth resulted in a slight reduction of ethanol yield ( $Y_{E/S}$ ), while no significant difference of yeast mass in glucose yield ( $Y_{X/S}$ ) was observed. The comparable value of  $Y_{X/S}$  shows that the *S. cerevisiae* strain used in the fermentation is still determined to grow and multiply the number of its cells at all the pH studied. As the fermentation pH increased from 3.0 to 5.0, the maximum yeast cells growth rate ( $\mu_{max}$ ) and the maximum ethanol production rate ( $q_{max}$ ) also increased. Lin et al. (2012) reported that at a low pH value (below 5.0) the main product of glucose fermentation is acetic acid (according to reaction 1).





As expected, more glucose was converted to ethanol at higher pH values (above 3.0) (Lin et al., 2012). In this study, the best fermentation condition was obtained at pH 5.0, which is in accordance with the report of Lee et al. (2011), Lin et al. (2012), Liu et al. (2015), and Malhotra and Basir (2020). The values of the average error of the calculated glucose and ethanol concentrations, which indicate their deviation from the corresponding experimental data were still acceptable as seen in Figure 4.

As shown in Figure 4, the experimental data and the corresponding glucose concentration calculation results possess a similar profile where glucose concentration in the fermentation broth drastically reduced to nearly zero at all fermentation pH in the first 16th hour. The concentration of  $H^+$ , which determines the pH of the fermentation broth affects the permeability of several important nutrients into the yeast cells yeast through the pores of the alginate matrix (Lee et al. 2011; Zabed et al., 2014). As a result, the ethanol concentration did not increase significantly up to 40 hours of fermentation and it became almost constant for the rest of the fermentation time.

This phenomenon proves that the pH value affects the vacuolar and cytosolic pH of the *S. cerevisiae* cells as well as the activity of plasma membrane ATPase (Peña et al., 2015).

Figure 4 exhibits a good agreement between the modeling results and the experimental data which suggests that the proposed model is quite good at describing the entire phenomena of the fermentation process. As seen in Figure 4 (a), the consumption of glucose available in the Na-Alginate beads surface at pH 3.0 was slower than at other fermentation conditions. This phenomenon can also be confirmed by the highest value of cell growth ( $K_{SX}$ ) and the rate of ethanol production ( $K_{SE}$ ; Table 3). Under extreme acidic fermentation conditions, the increase in intracellular pH reduces plasma permeability to protons and adenosine triphosphate (ATP) consumption, which in turn declines both glucose uptake and glycolytic activity (Woo et al., 2014).

#### 4. Conclusion

An unstructured fermentation model based on the phenomenological mechanisms involving the mass transfer and biochemical reaction of glucose by *S. cerevisiae* immobilized on Na-alginate beads for ethanol production has been successfully developed and satisfactorily validated using experimental data at various yeast mass loading, pH, and temperature with their average errors (%) were 7.21, 5.33, and 9.66, respectively. The mass transfer and biochemical reaction kinetics parameters obtained from this work can be applied in the design of the larger fermentation scale.

##### Author details

Astrilia Damayanti<sup>1</sup>  
 ORCID ID: <http://orcid.org/0000-0001-5724-0791>  
 Zuhriyan Ash Shiddieqy Bahlawan<sup>2</sup>  
 ORCID ID: <http://orcid.org/0000-0003-3872-4402>  
 Andri Cahyo Kumoro<sup>2</sup>  
 E-mail: [andrewkomoro@che.undip.ac.id](mailto:andrewkomoro@che.undip.ac.id)  
 ORCID ID: <http://orcid.org/0000-0001-9685-5406>  
<sup>1</sup> Department of Chemical Engineering, Faculty of Engineering, Universitas Negeri Semarang, Kampus Sekaran, Semarang, Indonesia.  
<sup>2</sup> Department of Chemical Engineering, Faculty of Engineering, Universitas Diponegoro, Soedarto, Indonesia.

##### NOMENCLATURE

$a_m$	specific surface area of microbial film ( $dm^{-1}$ )	$K_{EE}$	constant of ethanol production ( $g.dm^{-3}$ )
$CE_C$	critical ethanol concentration in liquid ( $g.dm^{-3}$ )	$K_{SX}$	constant in Monod equation of glucose ( $g.dm^{-3}$ )
		$CE_L$	ethanol concentration in liquid ( $g.dm^{-3}$ )
		$CG_L$	glucose concentration in liquid ( $g.dm^{-3}$ )
		$CG_{Li}$	glucose concentration in liquid interface ( $g.dm^{-3}$ )
		$CG_S$	glucose concentration in microbial film ( $g.dm^{-3}$ )
		$CG_{Si}$	glucose concentration in microbial interface ( $g.dm^{-3}$ )
		$H_S$	Henry's law like constant
		$k_{La}$	mass transfer coefficient from liquid to microbial film ( $dm.s^{-1}$ )

$K_{SE}$	constant in Monod equation of ethanol production ( $\text{g}\cdot\text{dm}^{-3}$ )
$q_{max}$	maximum specific ethanol production rate ( $\text{g}\cdot(\text{g}\cdot\text{h})^{-1}$ )
$r_E$	ethanol consumption rate ( $\text{g}\cdot\text{dm}^{-3}\cdot\text{s}^{-1}$ )
$r_G$	glucose consumption rate ( $\text{g}\cdot\text{dm}^{-3}\cdot\text{s}^{-1}$ )
$r_{Gm}$	glucose mass transfer rate ( $\text{g}\cdot\text{dm}^{-3}\cdot\text{s}^{-1}$ )
$r_x$	yeast cell growth rate ( $\text{g}\cdot\text{dm}^{-3}\cdot\text{s}^{-1}$ )
$m$	mass of yeast cell (g)
$t$	time (s)
$X$	yeast cell concentration ( $\text{g}\cdot\text{dm}^{-3}$ )
$Y_{E/S}$	yield coefficient in terms of ratio of the mass of ethanol production to the mass of glucose consumed
$Y_{X/S}$	yield coefficient in terms of ratio of mass of yeast cells growth to mass of glucose consumed
$V$	volume of microbial film
<b>Greek Symbol</b>	
$\delta$	thickness of microbial film (cm)
$\rho$	mass of <i>microorganisms</i> per volume of microbial film ( $\text{g}\cdot\text{cm}^{-3}$ )
$\mu_{max}$	maximum specific growth rate ( $\text{h}^{-1}$ )

#### Disclosure statement

No potential conflict of interest was reported by the author(s).

#### Funding

This work was supported by the Ministry of Research and Technology of the Republic of Indonesia for the financial support of this study through Hibah Penelitian Pasca Doktor (PDD) 2021 under contract [187-70/UN7.6.1/PP/2021].

#### Citation information

Cite this article as: Modeling of bioethanol production through glucose fermentation using *Saccharomyces cerevisiae* immobilized on sodium alginate beads, Astrilia Damayanti, Zuhriyan Ash Shiddieqy Bahlawan & Andri Cahyo Kumoro, *Cogent Engineering* (2022), 9: 2049438.

#### References

Aguilar-Uscanga, M. G., Garcia-Alvarado, Y., Gomez-Rodriguez, J., Phister, T., Delia, M. L., & Strehaiano, P. (2011). Modelling the growth and ethanol production of *Brettanomyces bruxellensis* at different glucose concentrations. *Letters in Applied Microbiology*, 53(2), 141–149. <https://doi.org/10.1111/j.1472-765X.2011.03081.x>

Azhar, S. H. M., & Abdulla, R. (2018). Bioethanol production from galactose by immobilized wild-type *Saccharomyces cerevisiae*. *Biocatalysis and Agricultural Biotechnology*, 14, 457–465. <https://doi.org/10.1016/j.bcab.2018.04.013>

Azhar, S. H. M., Abdulla, R., Jambo, S. A., Marbawi, H., Gansau, J. A., Faik, A. A. M., & Rodrigues, K. F. (2017). Yeasts in sustainable bioethanol production: A review. *Biochemistry and Biophysics Reports*, 10, 52–61. <https://doi.org/10.1016/j.bbrep.2017.03.003>

Bangrak, P., Limtong, S., & Phisalaphong, M. (2011). Continuous ethanol production using immobilized yeast cells entrapped in loofa-reinforced alginate carriers. *Brazilian Journal of Microbiology*, 42(2), 676–684. <https://doi.org/10.1590/S1517-83822011000200032>

Bird, R. B., Stewart, W. E., Lightfoot, E. N., & Klingenberg, D. J. (2015). *Introductory transport phenomena*. John Wiley & Sons, Inc.USA.

Beltran, G., Torija, M. J., Novo, M., Ferrer, N., Poblet, M., Guillamón, J. M., Rozès, N., & Mas, A. (2002). Analysis of yeast populations during alcoholic fermentation: A six year follow-up study. *Systematic and Applied Microbiology*, 25(2), 287–293. [10.1078/0723-2020-00097](https://doi.org/10.1078/0723-2020-00097)

Bušić, A., Mardetko, N., Kundas, S., Morzak, G., Belskaya, H., Šantek, M. I., Komes, D., Novak, S., & Šantek, B. Bioethanol production from renewable raw materials and its separation and purification: A review. (2018). *Food Technology and Biotechnology*, 56(3), 289–5546. <https://doi.org/10.17113/ftb.56.03.18.5546>

Beltran, G., Torija, M. J., Novo, M., Ferrer, N., Poblet, M., Guillamón, J. M., Rozès, N., & Mas, A. (2002). Analysis of yeast populations during alcoholic fermentation: A six-year follow-up study. *Systematic Applied Microbiology*, 25(2), 287–293. <https://doi.org/10.1078/0723-2020-00097>

Chacón-Navarrete, H., Martín, C., & Moreno-García, J. (2021). Yeast immobilization systems for second-generation ethanol production: Actual trends and future perspectives. *Biofuels, Bioproducts and Biorefining*, 15(5), 1549–1565. <https://doi.org/10.1002/bbb.2250>

Chen, H. Z., Liu, Z. H., & Dai, S. H. (2014). A novel solid-state fermentation coupled with gas stripping enhancing the sweet sorghum stalk conversion performance for bioethanol. *Biotechnology for Biofuels*, 7(53), 1–13. <https://doi.org/10.1186/1754-6834-7-53>

Damayanti, A., Kumoro, A. C., & Bahlawan, Z. A. S. Review calcium alginate beads as immobilizing matrix of functional cells: Extrusion dripping method, characteristics, and application. (2021). *IOP Conference Series: Materials Science and Engineering*, 1053(1), 012017. IOP publishing. <https://doi.org/10.1088/1757-899X/1053/1/012017>

Damayanti, A. S., Sediawan, W. B., & Sediawan, W. B. (2020). Biohydrogen production by reusing immobilized mixed culture in batch system. *International Journal of Renewable Energy Development*, 9(1), 37–42. <https://doi.org/10.14710/ijred.9.1.37-42>

Duarte, J. C., Rodrigues, J. A. R., Moran, P. J. S., Valença, G. P., & Nunhez, J. R. (2013). Effect of immobilized cells in calcium alginate beads in alcoholic fermentation. *AMB Express*, 3(31), 1–8. <https://doi.org/10.1186/2191-0855-3-31>

Eisenberg, T., & Büttner, S. (2014). Lipids and cell death in yeast. *FEMS Yeast Research*, 14(1), 179–197. <https://doi.org/10.1111/1567-1364.12105>

Estape, D., Godia, F., & Sola, C. (1992). Determination of glucose and ethanol effective diffusion coefficients in Ca-alginate gel. *Enzyme and Microbial Technology*, 14(5), 396–401. [https://doi.org/10.1016/0141-0229\(92\)90009-D](https://doi.org/10.1016/0141-0229(92)90009-D)

- Galaction, A. I., Lupășteanu, A. M., Turnea, M., & Cașcaval, D. (2010). Effect on internal diffusion on bioethanol production in a bioreactor with yeasts cells immobilized on mobile beds. *Environmental Engineering and Management Journal*, 9(5), 675–680. <https://doi.org/10.30638/eemj.2010.092>
- Gil, L. S., & Maupoey, P. F. (2018). An integrated approach for pineapple waste valorisation. Bioethanol production and bromelain extraction from pineapple residues. *Journal of Cleaner Production*, 172, 1224–1231. <https://doi.org/10.1016/j.jclepro.2017.10.284>
- Harcum, S. W., & Caldwell, T. P. (2020). High gravity fermentation of sugarcane bagasse hydrolysate by *Saccharomyces pastorianus* to produce economically distillable ethanol concentrations: Necessity of medium components examined. *Fermentation*, 6(1), 8. <https://doi.org/10.3390/fermentation6010008>
- Hossain, N., Zaini, J. H., & Mahlia, T. M. I. (2017). A review of bioethanol production from plant-based waste biomass by yeast fermentation. *International Journal of Technology*, 1(1), 5–18. <https://doi.org/10.14716/ijtech.v8i1.3948>
- Hu, X. H., Wang, M. H., Tan, T., Li, J. R., Yang, H., Leach, L., Zhang, R. M., & Luo, Z. W. (2007). Genetic Dissection of Ethanol Tolerance in the Budding Yeast *Saccharomyces cerevisiae*. *Genetics*, 175(3), 1479–1487. <https://doi.org/10.1534/genetics.106.065292>
- Huang, C. J., Lu, M. Y., Chang, Y. W., & Li, W. H. (2018). Experimental evolution of yeast for high-temperature tolerance. *Molecular Biology and Evolution*, 35(8), 1823–1839. <https://doi.org/10.1093/molbev/msy077>
- Karagoz, P., Bill, R. M., & Ozkan, M. (2019). Lignocellulosic ethanol production: Evaluation of new approaches, cell immobilization and reactor configurations. *Renewable Energy*, 143, 741–752. <https://doi.org/10.1016/j.renene.2019.05.045>
- Kostov, G., Popova, S., Gochev, V., Koprinkova-Hristova, P., Angelov, M., & Georgieva, A. (2012). Modeling of batch alcohol fermentation with free and immobilized yeasts *Saccharomyces Cerevisiae* 46 EVD. *Biotechnology & Biotechnological Equipment*, 26(3), 3021–3030. <https://doi.org/10.5504/BBEQ.2012.0025>
- Kuloyo, O. O., Du Preez, J. C., Del Prado García-aparicio, M., Kilian, S. G., Steyn, L., & Görgens, J. (2014). *Opuntia ficus-indica cladodes* as feedstock for ethanol production by *Kluyveromyces marxianus* and *Saccharomyces cerevisiae*. *World Journal of Microbiology and Biotechnology*, 30(12), 3173–3183. <https://doi.org/10.1007/s11274-014-1745-6>
- Kumoro, A. C., Damayanti, A., Bahlawan, Z. A., Melina, M., & Puspawati, H. Bioethanol production from oil palm empty fruit bunches using *Saccharomyces cerevisiae* immobilized on sodium alginate beads. (2021). *Periodica Polytechnica Chemical Engineering*, 65(4), 493–504. 16775. <https://doi.org/10.3311/PPch.16775>
- Kwolek-Mirek, M., & Zdrzag-Tecza, R. (2014). Comparison of methods used for assessing the viability and vitality of yeast cells. *FEMS Yeast Research*, 14(7), 1068–1079. <https://doi.org/10.1111/1567-1364.12202>
- Kyriakou, M., Chatziiona, V. K., Costa, C. N., Kallis, M., Koutsokeras, L., Constantinides, G., & Koutinas, M. (2019). Biowaste-based biochar: A new strategy for fermentative bioethanol overproduction via whole-cell immobilization. *Applied Energy*, 242, 480–491. <https://doi.org/10.1016/j.apenergy.2019.03.024>
- Landaeta, R., Acevedo, F., & Aroca, G. (2019). Effective diffusion coefficients and bioconversion rates of inhibitory compounds in flocs of *Saccharomyces cerevisiae*. *Electronic Journal of Biotechnology*, 42, 1–5. <https://doi.org/10.1016/j.ejbt.2019.08.001>
- Lee, K. H., Choi, I. S., Kim, Y. G., Yang, D. J., & Bae, H. J. (2011). Enhanced production of bioethanol and ultrastructural characteristics of reused *Saccharomyces cerevisiae* immobilized calcium alginate beads. *Bioresource Technology*, 102(17), 8191–8198. <https://doi.org/10.1016/j.biortech.2011.06.063>
- Lee, K. Y., & Mooney, D. J. (2012). Alginate: Properties and biomedical applications. *Progress in Polymer Science*, 37(1), 106–126. <https://doi.org/10.1016/j.proglolymsci.2011.06.003>
- Lee, S. Y., Park, J. M., & Kim, T. Y. (2011). Application of metabolic flux analysis in metabolic engineering. In C. Voigt (Ed.), *Synthetic biology, Part B - computer aided design and DNA assembly* (pp. 67–93). Elsevier Inc. <https://doi.org/10.1016/b978-0-12-385120-8.00004-8>
- Lee, J. S., Park, E. H., Kim, J. W., Yeo, S. H., & Kim, M. D. (2013). Growth and fermentation characteristics of *Saccharomyces cerevisiae* NK28 isolated from kiwi fruit. *Journal of Microbiology and Biotechnology*, 23(9), 1253–1259. <https://doi.org/10.4014/jmb.1307.07050>
- Lin, N. X., Xu, Y., & Yu, X. W. (2021). Overview of yeast environmental stress response pathways and the development of tolerant yeasts. *Systems Microbiology and Biomanufacturing*, 1–14. <https://doi.org/10.1007/s43393-021-00058-4>
- Liu, X., Jia, B., Sun, X., Ai, J., Wang, L., Wang, C., Zhao, F., Zhan, J., & Huang, W. (2015). Effect of initial pH on growth characteristics and fermentation properties of *Saccharomyces cerevisiae*. *Journal of Food Science*, 80(4), M800–M808. <https://doi.org/10.1111/1750-3841.12813>
- Liu, R., & Shen, F. (2008). Impacts of main factors on bioethanol fermentation from stalk juice of sweet sorghum by immobilized *Saccharomyces cerevisiae* (CICC 1308). *Bioresource Technology*, 99(4), 847–854. <https://doi.org/10.1016/j.biortech.2007.01>
- Malhotra, I., & Basir, S. F. (2020). Immobilization of invertase in calcium alginate and calcium alginate-kappa-carrageenan beads and its application in bioethanol production. *Preparative Biochemistry & Biotechnology*, 50(5), 494–503. <https://doi.org/10.1080/10826068.2019.1709979>
- Manheim, D. C., Detwiler, R. L., & Jiang, S. C. (2019). Application of unstructured kinetic models to predict microcystin biodegradation: Towards a practical approach for drinking water treatment. *Water Research*, 149, 617–631. <https://doi.org/10.1016/j.watres.2018.11.014>
- Mears, L., Stocks, S. M., Albaek, M. O., Sin, G., & Gernaey, K. V. (2017). Mechanistic fermentation models for process design, monitoring, and control. *Trends in Biotechnology*, 35(10), 914–924. <https://doi.org/10.1016/j.tibtech.2017.07.002>
- Mishra, A., Sharma, A. K., Sharma, S., Bagai, R., Mathur, A. S., Gupta, R. P., & Tuli, D. K. (2016). Lignocellulosic ethanol production employing immobilized *Saccharomyces cerevisiae* in packed bed

- reactor. *Renewable Energy*, 98, 57–63. <https://doi.org/10.1016/j.renene.2016.02.010>
- Murari, C. S., Machado, W. R. C., Schuina, G. L., & Del Bianchi, V. L. (2019). Optimization of bioethanol production from cheese whey using *Kluyveromyces marxianus* URM 7404. *Biocatalysis and Agricultural Biotechnology*, 20, 101182. <https://doi.org/10.1016/j.bcab.2019.101182>
- Najafpour, G., Younesi, H., Syahidah, K., & Ismail, K. (2004). Ethanol fermentation in an immobilized cell reactor using *Saccharomyces cerevisiae*. *Bioresource Technology*, 92(3), 251–260. <https://doi.org/10.1016/j.biortech.2003.09.009>
- Nikolić, S., Mojović, L., Rakin, M., Pejini, J., Djukić-Vuković, A., & Bulatović, M. (2012). Simultaneous enzymatic saccharification and fermentation (SSF) in bioethanol production from corn meal by free and immobilized cells of *Saccharomyces cerevisiae* var. *ellipsoideus*. *Journal of Chemical Science and Technology*, 1(1), 21–26.
- Nordmeier, A., & Chidambaram, D. (2018). Use of *Zymomonas mobilis* immobilized in doped calcium alginate threads for ethanol production. *Energy*, 165, 603–609. <https://doi.org/10.1016/j.energy.2018.09.137>
- Nuanpeng, S., Thanonkeo, S., Klanrit, P., & Thanonkeo, P. (2018). Ethanol production from sweet sorghum by *Saccharomyces cerevisiae* DBKKUY-53 immobilized on alginate-loofah matrices. *Brazilian Journal of Microbiology*, 49(1), 140–150. <https://doi.org/10.1016/j.bjm.2017.12.011>
- Peña, A., Sánchez, N. S., Álvarez, H., Calahorra, M., & Ramirez, J. (2015). Effects of high medium pH on growth, metabolism and transport in *Saccharomyces cerevisiae*. *FEMS Yeast Research*, 15(2). <https://doi.org/10.1093/femsyr/fou005>
- Phisalaphong, M., Srirattana, N., & Tanthapanichakoon, W. (2006). Mathematical modeling to investigate temperature effect on kinetic parameters of ethanol fermentation. *Biochemical Engineering Journal*, 28(1), 36–43. <https://doi.org/10.1016/j.bej.2005.08.039>
- Rastogi, M., & Shrivastava, S. (2017). Recent advances in second generation bioethanol production: An insight to pretreatment, saccharification and fermentation processes. *Renewable and Sustainable Energy Reviews*, 80, 330–340. <https://doi.org/10.1016/j.rser.2017.05.225>
- Rattanapan, A., Limtong, S., & Phisalaphong, M. (2011). Ethanol production by repeated batch and continuous fermentations of blackstrap molasses using immobilized yeast cells on thin-shell silk cocoons. *Applied Energy*, 88(12), 4400–4404. <https://doi.org/10.1016/j.apenergy.2011.05.020>
- Riley, M. R., Muzzio, F. J., Buettner, H. M., & Reyes, S. C. (1996). A simple correlation for predicting effective diffusivities in immobilized cell systems. *Journal of Biotechnology and Bioengineering*, 49(2), 223–227. <https://doi.org/10.1002/bit.260490202>
- Saha, K., Verma, P., Sikder, J., Chakraborty, S., & Curcio, S. (2019). Synthesis of chitosan-cellulase nanohybrid and immobilization on alginate beads for hydrolysis of ionic liquid pretreated sugarcane bagasse. *Renewable Energy*, 133, 66–76. <https://doi.org/10.1016/j.renene.2018.10.014>
- Scott, C. D., Woodward, C. A., & Thompson, J. E. (1989). Solute diffusion in biocatalyst gel beads containing biocatalysis and other additives. *Enzyme and Microbial Technology*, 11(5), 258–263. [https://doi.org/10.1016/0141-0229\(89\)90040-9](https://doi.org/10.1016/0141-0229(89)90040-9)
- Silva-Illanes, F., Tapia-Venegas, E., Schiappacasse, M. C., Trably, E., & Ruiz-Filippi, G. (2017). Impact of hydraulic retention time (HRT) and pH on dark fermentative hydrogen production from glycerol. *Energy*, 141, 358–367. <https://doi.org/10.1016/j.energy.2017.09.073>
- Sivarathnakumar, S., Jayamuthunagai, J., Baskar, G., Praveenkumar, R., Selvakumari, I. A. E., & Bharathiraja, B. (2019). Bioethanol production from woody stem *Prosopis juliflora* using thermo tolerant yeast *Kluyveromyces marxianus* and its kinetics studies. *Bioresource Technology*, 293, 122060. <https://doi.org/10.1016/j.biortech.2019.122060>
- Stanley, D., Bandara, A., Fraser, S., Chambers, P. J., & Stanley, G. A. (2010). The ethanol stress response and ethanol tolerance of *Saccharomyces cerevisiae*. *Journal of Applied Microbiology*, 109(1), 13–24. <https://doi.org/10.1111/j.1365-2672.2009.04657.x>
- Tkavc, R., Matrosova, V. Y., Grichenko, O. E., Gostinčar, C., Volpe, R. P., Klimenkova, P., Gaidamakova, E. K., Zhou, C. E., Stewart, B. J., Lyman, M. G., Malfatti, S. A., Rubinfeld, B., Courtot, M., Singh, J., Dalgard, C. L., Hamilton, T., Frey, K. G., Gunde-Cimerman, N., Dugan, L., & Daly, M. J. (2018). Prospects for fungal bioremediation of acidic radioactive waste sites: Characterization and genome sequence of *Rhodotorula taiwanensis* MD1149. *Frontiers in Microbiology*, 8, 2528. <https://doi.org/10.3389/fmicb.2017.02528>
- Todhanakasem, T., Wu, B., & Simeon, S. (2020). Perspectives and new directions for bioprocess optimization using *Zymomonas mobilis* in the ethanol production. *World Journal of Microbiology and Biotechnology*, 36(8), 1–16. <https://doi.org/10.1007/s11274-020-02885-4>
- Tofighi, A., Assadi, M. M., Asadirad, M. H. A., & Karizi, S. Z. (2014). Bio-ethanol production by a novel autochthonous thermo-tolerant yeast isolated from wastewater. *Journal of Environmental Health Science and Engineering*, 12(1), 1–6. <https://doi.org/10.1186/2052-336X-12-107>
- Ünal, M. Ü., Chowdhury, G., & Şener, A. (2020). Effect of temperature and nitrogen supplementation on bioethanol production from waste bread, watermelon and muskmelon by *Saccharomyces cerevisiae*. *Biofuels*, 1–5. <https://doi.org/10.1080/17597269.2020.1724440>
- Vives, C., Casas, C., Gdia, F., & Sola, C. (1993). Microbiology biotechnology determination of the intrinsic fermentation kinetics of *Saccharomyces cerevisiae* cells immobilized in Ca-alginate beads and observations on their growth. *Applied Microbiology and Biotechnology*, 38(4), 467–472. <https://doi.org/10.1007/BF00242939>
- Woo, J.-M., Yang, K.-M., Kim, S.-U., Blank, L. M., & Park, J.-B. (2014). High temperature stimulates acetic acid accumulation and enhances the growth inhibition and ethanol production by *Saccharomyces cerevisiae* under fermenting conditions. *Applied Microbiology and Biotechnology*, 98(13), 6085–6094. <https://doi.org/10.1007/s00253-014-5691-x>

- Zabed, H., Faruq, G., Sahu, J. N., Azirun, M. S., Hashim, R., & Nasrulhaq Boyce, A. (2014). Bioethanol production from fermentable sugar juice. *The Scientific World Journal*, 2014, 1–12. <https://doi.org/10.1155/2014/957102>
- Zakhartsev, M., & Reuss, M. (2018). Cell size and morphological properties of yeast *Saccharomyces cerevisiae* in relation to growth temperature. *FEMS Yeast Research*, 18(6), 1–16. <https://doi.org/10.1093/femsyr/foy052>
- Zentou, H., Abidin, Z. Z., Yunus, R., Biak, D. R. A., Issa, M. A., & Pudza, M. Y. (2021). A new model of alcoholic fermentation under a by-product inhibitory effect. *ACS Omega*, 6(6), 4137–4146. <https://doi.org/10.1021/acsomega.0c04025>
- Zentou, H., Abidin, Z. Z., Yunus, R., Biak, D. R. A., & Korelskiy, D. (2019). Overview of alternative ethanol removal techniques for enhancing bioethanol recovery from fermentation broth. *Processes*, 7(7), 458. <https://doi.org/10.3390/pr7070458>
- Žur, J., Wojcieszynska, D., & Guzik, U. (2016). Metabolic responses of bacterial cells to immobilization. *Molecules*, 21(7), 958. <https://doi.org/10.3390/molecules21070958>



© 2022 The Author(s). This open access article is distributed under a Creative Commons Attribution (CC-BY) 4.0 license.

You are free to:

Share — copy and redistribute the material in any medium or format.

Adapt — remix, transform, and build upon the material for any purpose, even commercially.

The licensor cannot revoke these freedoms as long as you follow the license terms.

Under the following terms:

Attribution — You must give appropriate credit, provide a link to the license, and indicate if changes were made.

You may do so in any reasonable manner, but not in any way that suggests the licensor endorses you or your use.

No additional restrictions

You may not apply legal terms or technological measures that legally restrict others from doing anything the license permits.

***Cogent Engineering* (ISSN: 2331-1916) is published by Cogent OA, part of Taylor & Francis Group.**

**Publishing with Cogent OA ensures:**

- Immediate, universal access to your article on publication
- High visibility and discoverability via the Cogent OA website as well as Taylor & Francis Online
- Download and citation statistics for your article
- Rapid online publication
- Input from, and dialog with, expert editors and editorial boards
- Retention of full copyright of your article
- Guaranteed legacy preservation of your article
- Discounts and waivers for authors in developing regions

**Submit your manuscript to a Cogent OA journal at [www.CogentOA.com](http://www.CogentOA.com)**

